Hindawi
Advances in Civil Engineering
Volume 2020, Article ID 3183206, 14 pages
https://doi.org/10.1155/2020/3183206

Research Article

Experimental Study on Hysteretic Behavior of Double-Plate Reinforced Overlapped K-Joints

Wenwei Yang,[1] Shuntao Li,[1] Ruhao Yan,[1] and Yaqi Suo[2]

[1]*School of Civil and Hydraulic Engineering, Ningxia University, Yinchuan 750021, China*
[2]*School of Civil Engineering, Southeast University, Nanjing 211100, China*

Correspondence should be addressed to Shuntao Li; lishuntaoqqq@live.com

Received 18 August 2019; Revised 13 November 2019; Accepted 18 November 2019; Published 3 January 2020

Academic Editor: Alessandro Palmeri

The lifetime of hollow section tubular joints frequently can be shortened owing to the occurrence of the welded cracks and the plastic deformation of chords under the cyclic loading, because of the deficient radial bearing capacity of the steel tube. To avoid such failures, this paper proposes a novel method to strengthen the chord with double plates at the intersection of the chord and braces. To further investigate the efficiency of this strengthening method on hysteretic performance and energy depletion ability of the overlapped K-joints with hollow sections, two unreinforced K-joints and two reinforced K-joints were fabricated. By loading on the braces with collaborative cyclic loading, the joints failure modes, hysteresis curve, and skeleton curve were obtained. The bearing capacity, ductility, and energy depletion of the joints were assessed and the restoring force model of joints was proposed. The results show that the failure mode of the unreinforced joint is the plastic failure of the surface of the chord. For the K-RC1 (double-plate reinforced square hollow section tubular K-joints), cracks appeared at the junction weld between the through brace and the overlapped brace. However, cracks extended along the weld at the intersection of the chord and the through brace for K-CC1 (double-plate reinforced circular hollow section tubular K-joints). There is no obvious deformation on the chord surface of reinforced joints. Experimental results reveal that the mechanical properties of the joints can be improved effectively by such reinforcement measures and that the plastic deformation of the chord can also be restrained. Meanwhile, the reinforcement measures demonstrate the ability to avoid the risk of large stress concentration of the chord in the area where the braces and chords are intersected. The bearing capacity of the joint was increased; however, the ductility of the joint was weakened.

1. Introduction

Hollow structural sections are characterized by light weight and high strength, excellent axial compression resistance and torque resistance, and beautiful artistic modeling, among others [1, 2]. Hence, hollow structural sections have been widely used in many popular structures such as terminal buildings, bridges, and large sports centers, in which circle, square, and ellipse are the primary shapes [3]. The lifetime of hollow section tubular joints frequently is shortened by the occurrence of the corrosion [4, 5], welded cracks [6], and the plastic deformation of chords under the cyclic loading because of the deficient radial bearing capacity of the steel tube [1, 7]. Relevant design specifications and guidelines for reinforced steel joints have also been proposed accordingly [8, 9]. As one of the most widely used steel tubular truss joints in the field of the building structure, overlapped K-joints are generated in the actual construction process of the steel tubular truss when two braces (overlap brace and through brace) intersect on the surface of a chord. There are many additional factors that affect the mechanical behavior of the overlapped joints, including the geometric parameter of the joints, the shape of brace and chord (circular, square, or rectangular), different reinforcement measures, and the hidden weld [10]. In overlapped K-joints, the overlap of the intersections of the brace (hidden invisible) can be welded to the chord or not welded [11]. Compared to the joints that do not weld the hidden welds, the joints of the welded hidden welds have the better bearing capacity, but the ductility and hysteresis performance are

reduced [12]. Nevertheless, Chinese Code of Steel Structures Design does not specify whether such welds should be welded or not [13].

If the hidden weld of overlapped K-joint is welded, it must be welded according to the welding sequence before the overlapped brace is assembled, which is difficult to achieve in the actual construction process. Based on this situation, the hidden welds of overlapped K-joints are usually not welded. However due to the lack of stiffness of the chord members, it is easy to cause plastic deformation of the circular hollow steel tubular truss (CHS). To prevent this unfavorable situation from happening on the unreinforced tubular joints, scholars have adopted different approaches such as pouring concrete into the steel tube [14], adding a double-plate outer chord [15] and adopting internal ring stiffeners [16]. Although the strengthening methods mentioned above have improved the bearing capacity of joints in varying degrees, there are also some new problems to be introduced. In-filled concrete in steel pipes can improve the bearing capacity and rigidity of the joints [17, 18] and also can better resist impact [19]; however, pouring concrete into the chords increases self-weight of joints and introduces additional construction problems such as debonding and voids [20]. Additionally, many studies [21–23] have shown that adopting internal ring stiffeners can effectively increase the static strength of the joints, which made the process of specimens' preparation cumbersome. In summary, the reinforced joints with a double plate are very convenient and fast. It is to weld the cross brace to the double plate and then to weld the double plate on the steel tubular truss [24]. For example, some scholars [25, 26] have proposed to use the same thickness for the reinforcement plate and the chord for more economical purposes.

At present, there are many static studies for the CHS K-joints. Kurobane et al. summarized a large amount of data on the results of tubular joint experiments [27]. Zhao et al.'s research on overlapped CHS K-joints [28] shows that whether the hidden weld has no significant influence on the bearing capacity of the K-joints, but it will affect the failure mode. Kim [29] proposed a new bearing capacity formula for the K-joints. In addition, many researchers [30–37] have carried out experimental studies on different types of steel tube joints and obtained many valuable conclusions.

It can be seen from the above statements that it is not difficult to find that the static behavior of reinforced or unreinforced joints has been studied in detail. At the same time, the hysteretic performance of the joints also represents the energy dissipation performance [38–41], when the structure is subjected to earthquake or other vibrations. Compared to the static performance of joints, the research on joints hysteresis performance is rare, but it is very important to evaluate the joints. According to references [1, 42–44], the authors carried out the experimental tests on the hysteretic behavior of unreinforced joints and the results showed that the weld toe cracking is the main failure mode of unreinforced joints. In reference [24], through the hysteretic behavior test of tubular joints strengthened by double steel plate and filled concrete, it is found that although such a reinforcement pattern can greatly increase the bearing capacity of the joints, the ductility is actually reduced. In this paper, to further investigate the efficiency of this strengthening method on hysteretic performance and energy depletion ability of the overlapped K-joints, four overlapped K-joints under coordinated cyclic loading are experimentally studied. The failure modes, hysteresis curves, and skeleton curves of the joints were obtained. The bearing capacity, ductility, and energy depletion of the joints were estimated quantitatively, and the restoring force model of the joints is proposed based on this.

2. Experimental Design

2.1. Specimens Design. Two unreinforced overlapped K-joints and two double plates reinforced overlapped K-joints were designed in this test, according to the design guidelines [45]. First, weld the through brace to the chord, then weld the overlapped brace to the through brace and the chord. For reinforced joints, the plate was welded to the chord by surrounding welding, and then two braces were welded to the plate. Design of the overlapped K-joints is shown in Figure 1. In addition to the double plate, Q345 steel was used in the chords and braces. As shown in Table 1, "K-RC" means that the chord of the overlapped K-joint is square and the brace is circular, and "K-CC" means that the chord and brace are both circular. Geometrical dimensions of the chord and brace cross section were defined as $D(B) \times T$ and $d \times t$, respectively, as well as the double plate $D_0(B_0) \times T_0$. L_c and L were the length of chord and double plate, respectively. L_b was the vertical length of the brace. θ is the angle between the axis of brace and chord. e is eccentricity, which is the distance between the axis of a chord and the intersection point of double braces' axes($\alpha = 2L_c/D(B)$, $\beta = d/D(B)$, $\gamma = D(B)/(2T)$, $\tau = t/T$).

2.2. Material Properties. Steels of different specifications are made into three standard samples of each group and standard tensile tests are carried out to determine the material properties of the steel members [46]. Finally, the results, including the yield strength (f_y), tensile strength (f_u), yield strain (ε_y), elongation (δ), and elasticity modulus (E), are shown in Table 2. In addition, the yielding strength and ultimate strength of the double plate is 368.7 MPa and 526.8 MPa.

2.3. Test Program. The loading devices used in the test include reaction frame, upright column, cross beam, transfer beam, test system, and loading system, as shown in Figure 2. The specimens were placed in a common plane with the reaction frame and the left end plate of chord was fixed with the transfer beam and the right end plate was a sliding support. Two braces were articulated along their axis with two hydraulic jacks, which can provide tension and compression for 500 kN, respectively. The reciprocating load was exerted on the end plate of the braces by hydraulic jacks. That is, the magnitude of the load applied to the through brace and the overlapped brace is synchronous.

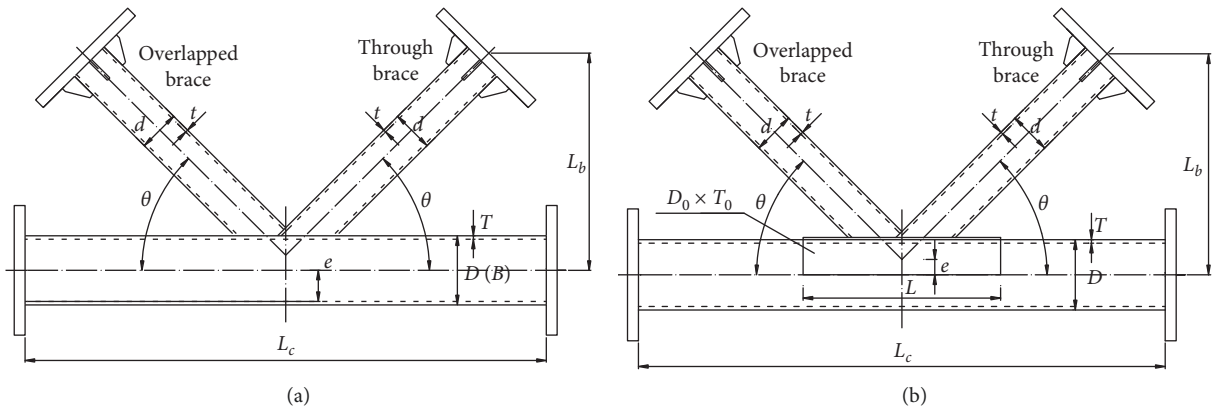

Figure 1: Design of the overlapped K-joints. (a) K-RC or K-CC. (b) K-RC1or K-CC1.

Table 1: Geometrical parameters of the overlapped K-joints.

Specimen	L_c (mm)	L_b (mm)	$D(B) \times T$ (mm)	$d \times t$ (mm)	L (mm)	$D_0(B_0) \times T_0$ (mm)	θ	e (mm)	α	β	Γ	τ
K-RC	1200	450	200 × 8	95 × 5	—	—	45°	55	12	0.48	12.5	0.63
K-RC1	1200	450	200 × 8	95 × 5	450	212 × 6	45°	55	12	0.48	12.5	063
K-CC	1200	450	159 × 6	89 × 5	—	—	45°	35	15.1	0.56	13.3	0.83
K-CC1	1200	450	159 × 6	89 × 5	450	171×6	45°	35	15.1	0.56	13.3	0.83

Table 2: Test result of steel tubular material properties.

Specification	f_y (MPa)	f_u (MPa)	E (GPa)	$\varepsilon_y = f_y/E$	f_u/f_y	δ (%)
200 × 200 × 8	391.1	533.0	226.2	0.0017	1.36	35.3
95 × 5	377.6	515.6	214.6	0.0017	1.37	25.9
159 × 6	386.5	531.5	222.4	0.0017	1.38	34.2
89 × 5	373.1	510.1	210.2	0.0018	1.37	26.6

To eliminate the installation gap and check whether the instrument is normal, a 25%-yield load was applied to the specimen before formal loading. The force-displacement hybrid loading mode was adopted, and the loading scheme is shown in Figure 3. The formal loading is divided into two stages: the first stage was force-controlled with three levels and the increment of each stage was 25% of the yield load with two circulations. The second stage was displacement-controlled. When the first stage is completed, the displacement Δy corresponding to the yield load of the brace is taken as the increment. Each level load circulated three times, until the specimen failure.

The measurement contents of the test include reaction force, displacement, local deformation of the specimen, stress distribution of brace, and strain distribution of the specimen. Each joint test specimen was equipped with five displacement transducers, 16 strain gauges, and 16 strain rosettes for simultaneous data acquisition. The layout of strain gauge and displacement transducer is shown in Figure 4. Each specimen is equipped with strain gauge and T1–T16 strain rosettes to monitor the strain in the complex area, the distance of which from the weld was 20 mm. Strain rosettes were arranged parallel to the weld lines. The S1–S8 strain gauges were arranged in the circumferential direction of the brace and, respectively, located on the line 60 mm from line 1 and line 2. The S9–S16 strain gauges were arranged in the circumferential direction of the chord and located on the line 150 mm from the parallel line 3. The displacement transducers D1–D4 were used to monitor deformation of the braces relative to chord, which were installed on the top surface of the square chord, which were located on the line 50 mm from the parallel line 3. The displacement transducer D5 monitored the deformation of the chord's bottom, which were located on the bottom surface of the square chord or circular chord.

3. Analysis of Experimental Results

3.1. Failure Modes. The failure modes of the specimens are shown in Figure 5. The specimens are in the elastic status before yielding and there is no obvious deformation of the chords and braces. With the increase of load, the failure modes of the specimens were different after yielding.

In the process of collaborative cyclic loading, the failure mode of K-RC and K-CC specimens without reinforcement can be divided into two stages namely: chord yielding and local cracking. With the increase of cyclic loading, the concave and convex deformation on the surface of the chords appears gradually as yield strength of the unreinforced joints being reached, due to different stress states imposed by the brace, as shown in Figures 5(a) and 5(c). The failure modes of the reinforced joints and the unreinforced joints were very different. In terms of the K-RC1 joint, first of all, the cracks appeared along the weld at the intersection of

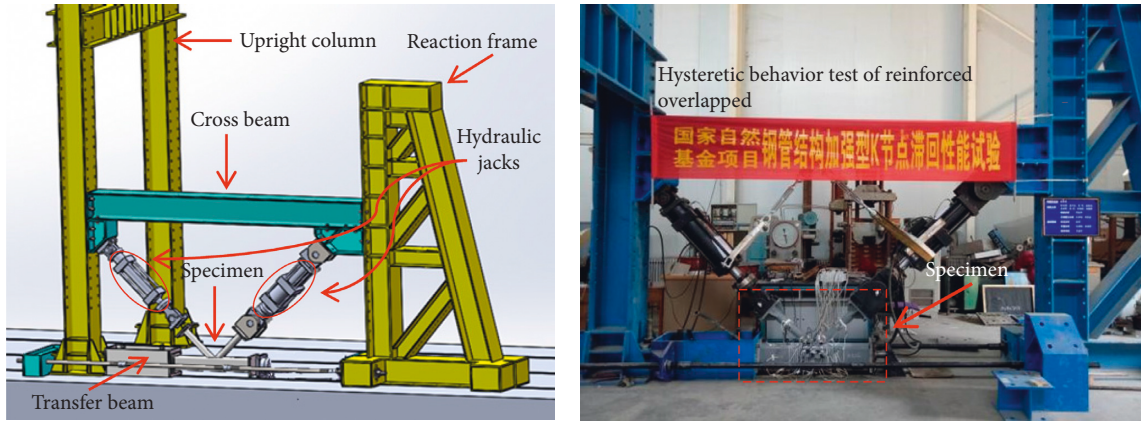

(a) (b)

Figure 2: Loading device.

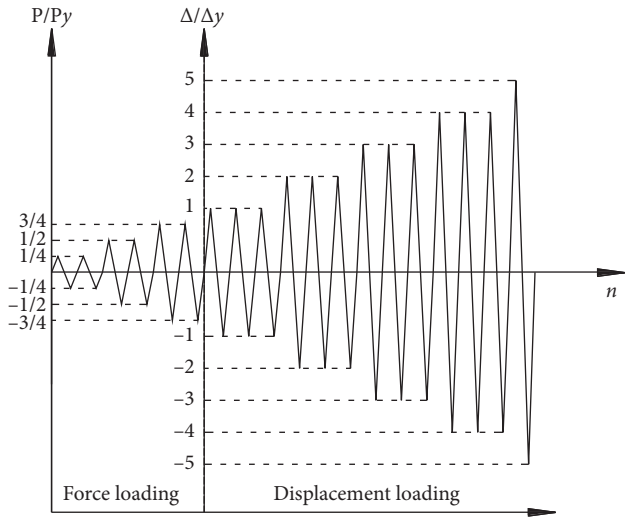

Figure 3: Loading scheme.

the two braces and then the crack propagated along the weld to the saddle point (A point), with a faster-spreading speed than before, as shown in Figure 5(b). As for K-CC1 joint, the failure mode can be divided into two stages, namely, initial cracking and crack propagation. Cracks firstly appeared at point B under collaborative cyclic loading and then extended along the weld at the intersection of the chord and the through brace to point C, which is shown in Figure 5(d). In general, great changes have taken place in the failure modes of the joints reinforced by the double plate. The reinforcement measure of the double plate can significantly increase the mechanical properties of the K-joints, restrain the plastic deformation of the chord, and avoid the large stress concentration of the chord in the area where the braces and chords intersect.

It is well known that repeated loads tend to cause local buckling of the structure leading to brittle failure. Furthermore, the stiffness of steel tube at weld connection is not continuous, which may become stress raisers leading to cracking in the weld toe. Such high stress raisers are also the main cause of brittle failure in this area and the welding quality also causes brittle failure, because in the process of welding the chord and the brace, a large welding residual tensile stress is generated along the direction of the weld toe, which causes such a welded joint to cause such brittle failure at the weld region. The experimental tests on the four specimens have verified the above discussion. After a period of loading, cracks could be observed at the welding seam at the intersection of a chord and brace, extending along the weld, which is coincident with the failure modes shown in Figures 5(a)–5(d).

3.2. Hysteretic Curve. In order to evaluate the seismic capacity of overlapped K-joints under collaborative cyclic loading, it is essential to evaluate the hysteretic performance of the K-joints by the load-displacement curves. The hysteretic curves of the test specimens are shown in Figure 6. The longitudinal axis is the load P exerted by the hydraulic jack, as shown in Figure 6, and the load of through brace is a positive number in tension and negative number in compression. The transverse axis is the axial displacement δ of the through brace, whose direction is the same as that of P.

By analyzing the hysteretic curves of the K-joints under the reciprocating load, the following characteristics were observed: (1) the stiffness of joints hardly decreases until the weld cracks occur, which can be seen in Figure 6. The area enveloped by the hysteretic curves is very small, and the hysteretic curves are narrow and slender in the elastic stage; the stiffness of the joints changes little, there is hardly residual deformation and the energy dissipating capacity of joints is poor. After yielding, the joints entered the inelastic stage, the slope of hysteretic curve decreased, the stiffness of the joints degenerated, and the area enveloped by the hysteretic loop increased gradually. (2) Compared to the reinforced joints with double plate, the hysteretic curves of the unreinforced joints have better plumpness and better energy dissipating capacity. Furthermore, there is a "pinch" phenomenon in the hysteretic curves of double-plate reinforced overlapped K-joints. (3) For reinforcement joints

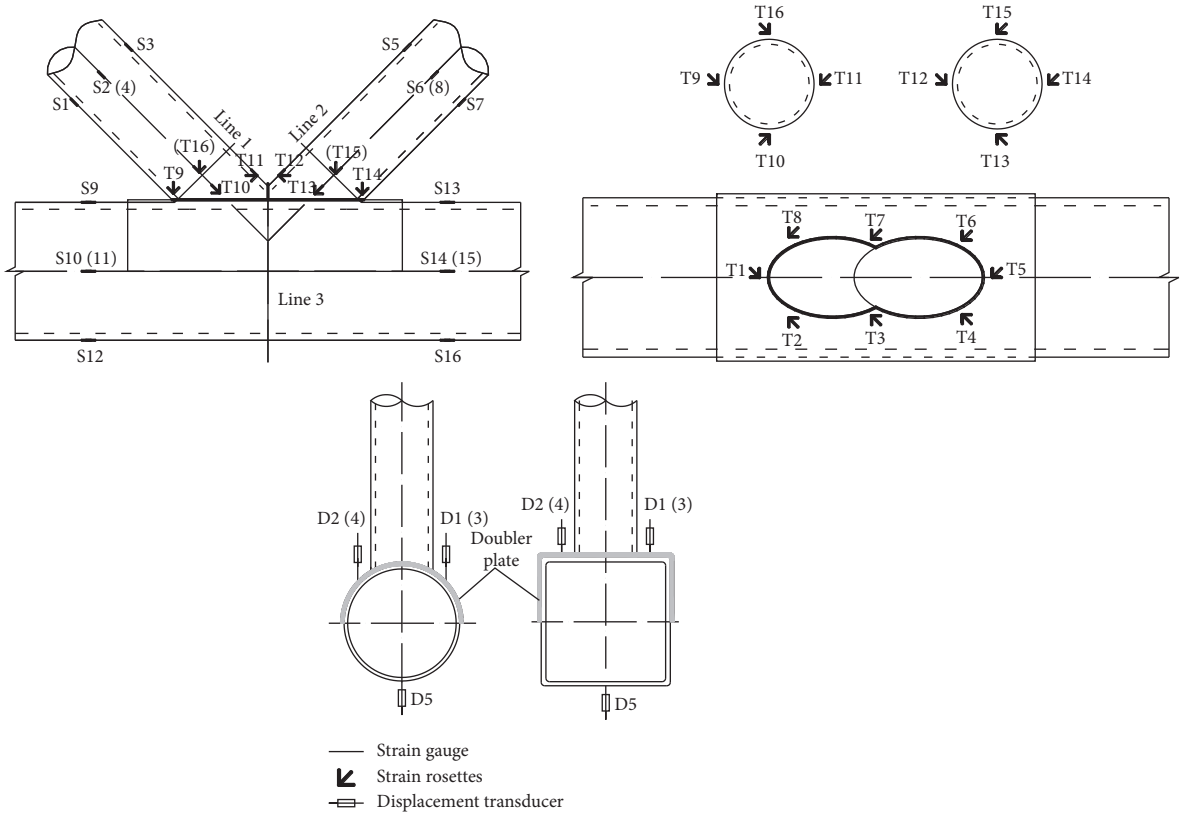

Figure 4: Measurement points of specimen.

K-RC1 and K-CC1, the area of the hysteretic loop under tension is smaller than that under compression with the increase of cyclic displacement, which indicates that the braces under compression enter the energy dissipating stage earlier than the braces under tension. On the contrary, the areas of hysteretic loops with unreinforced joints are approximately equal under tension and compression.

The bearing capacity increased continuously before the specimen yields. The comparison results of the bearing capacity of each joint are shown in Table 3. The ratios of tensile ultimate load and compression ultimate load of reinforced and unreinforced joints are defined as r_t and r_c, respectively. Compared to the unreinforced joints, the ultimate bearing capacity of the reinforced joints is higher. For instance, the maximum tensile load and compressive load of the K-RC1 are 16.8% and 63.5% higher than that of the joints K-RC, and the maximum tensile load and compressive load of K-RC1 are 13.9% and 95.0% higher than that of the joints K-CC, respectively. In terms of the unreinforced joints, the bearing capacity of both K-RC is slightly higher than that of the K-CC. Conversely, the bearing capacity of the K-RC1 both is smaller than that of the K-CC1. The above discussion shows that the hysteretic behavior and load-bearing capacity of overlapped K-joints with different cross section forms, strengthened by double plate, are different.

3.3. Skeleton Curve and Ductility Coefficient. The skeleton curves of the joints are plotted in the same coordinate system as shown in Figure 7. As can be seen from the figure, the load-displacement curve is approximated to a straight line when the joint is in the elastic status. With the increase of cyclic displacement, the unreinforced joints enter the inelastic stage earlier than the double-plate reinforced joints. In the experiment, the plate was welded to the chord only by surrounding welding, and the intermediate bonding surface was not welded. Therefore, under cyclic loading, the deformation of the plate causes a slight separation between the plate and the chord, which is why the initial stiffness of the reinforced joint is smaller than that of the unreinforced joint. Of course, this also makes the deformation capacity of the reinforced joints better.

The double-plate reinforcement has improved the strength of the overlapped K-joints and the improvement of compressive capacity is more obvious. The ultimate capacity P_u in tension of the K-RC1 and K-CC1 are, respectively, 16.8% and 13.9% higher than the K-RC and K-CC. However, the ultimate capacity P_u in compression of the K-RC1 and K-CC1 are, respectively, 63.5% and 95.0% higher than the K-RC and K-CC. The above phenomenon is caused by the closure of cracks in the braces of the joints under compression. Hence, the compressive strength of joints increases more than the tensile strength. As far as the section form of the chord is concerned, the difference between the ultimate capacity in tension and compression of K-RC and K-CC is not more than 5%. The tensile and compressed yield load (P_y) of K-RC are 17.8% and 10.5% higher than that of the joints K-CC, while the tensile and compressive yield load(P_y) of K-RC1 are 20.1% and 18.6% smaller than that of the joints K-CC1.

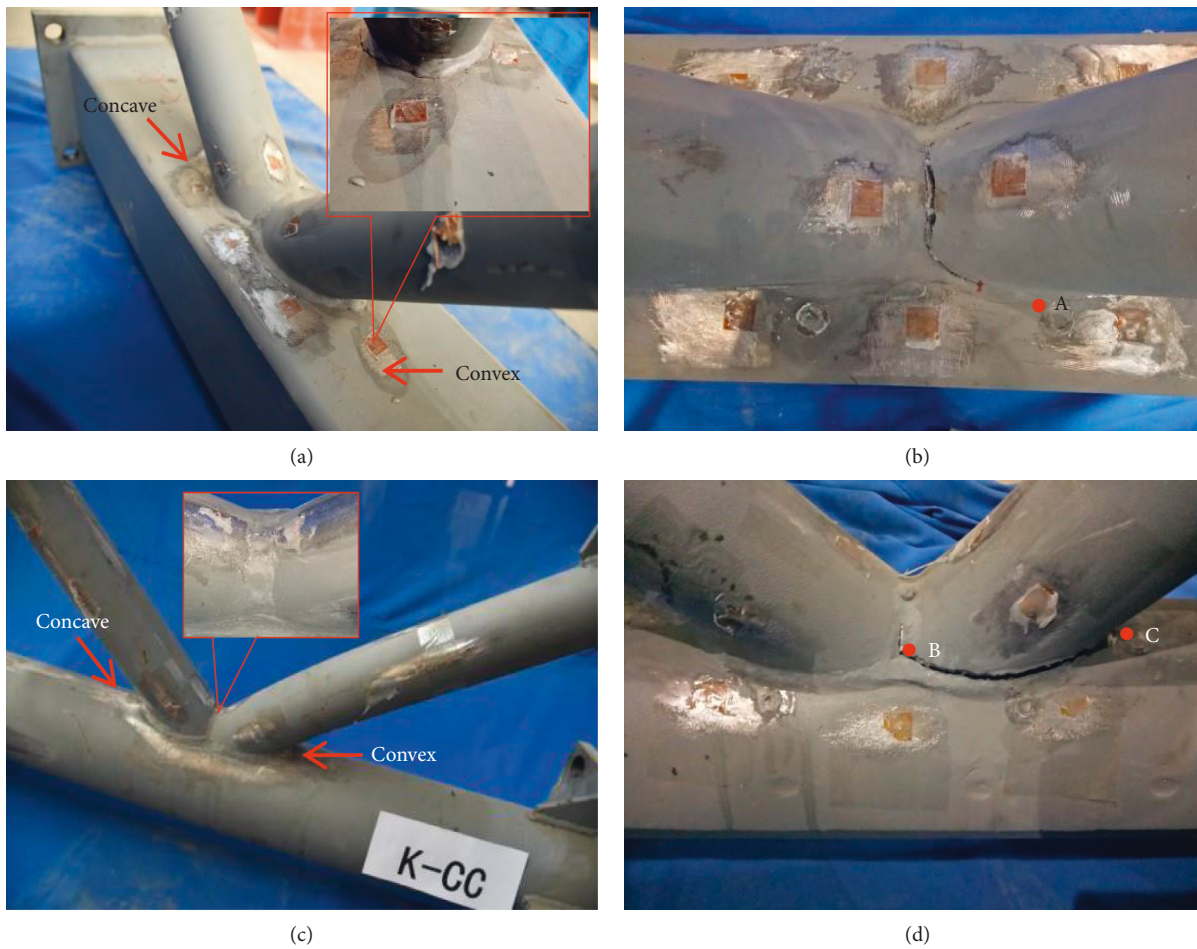

Figure 5: The failure modes of the specimens. (a) K-RC, (b) K-RC1, (c) K-CC, and (d) K-CC1.

The ductility of the structure determines its seismic capacity and the displacement ductility ratio μ is used to evaluate the deformability of the K-joints. The ductility coefficient μ is defined as δ_u/δ_y, δ_u, and δ_y are the ultimate displacement and the yield displacement of a joint, respectively, [1] and the calculation results of μ are shown in Table 3. As shown in the calculation results, the displacement ductility coefficient of unreinforced joints are almost equal, as well as the reinforced joints. Furthermore, the displacement ductility coefficients of unreinforced joints are about 1.3 times of those of K-RC1 and K-CC1. The yield displacement and ultimate displacement of reinforced joints are obviously larger than those of unreinforced joints. In terms of seismic resistance, the ultimate bearing capacity of the double-plate reinforced joints are significantly increased, while the deformation capacity of the joints are slightly reduced. Therefore, for the seismic resistance of double-plate reinforced K-joints, this reinforcement is still an effective and worthwhile reinforcement.

3.4. Energy Dissipation. Energy dissipation capacity is an important index in evaluation of mechanical properties of the K-joints. The energy dissipating capacity of joints is measured by the area enveloped by P-δ hysteretic curves. In this paper, the energy dissipation factor η_a is used as the evaluation index of earthquake resistance of the K-joints, which is defined as the following equation (1). As shown in Figure 8, where S_{ABC} and S_{CDA} are the total area surrounded by the hysteresis curve of the outermost circle, that is, the sum of tensile energy and compression energy. S_{OBE} and S_{ODF} are the dissipated linear energy in tensile and compressive stages, respectively. Furthermore, the equivalent viscous damping ratio (h_e) is introduced, which is shown in equation (2).

$$\eta_a = \frac{S_{ABC} + S_{CDA}}{S_{\Delta OBE} + S_{\Delta ODF}}, \tag{1}$$

$$h_e = \frac{\eta_a}{2\pi}. \tag{2}$$

In addition, the cumulative energy dissipation coefficient E_T and the cumulative energy dissipation ratio η are introduced to measure the cumulative energy dissipation during the whole loading process. The relevant formulas are shown below:

$$E_T = \sum_{i=1}^{n} \left(E_i^+ + E_i^-\right), \tag{3}$$

$$\eta = \frac{E_T}{E_y}, \tag{4}$$

$$E_y = \frac{P_y \times \delta_y}{2}. \tag{5}$$

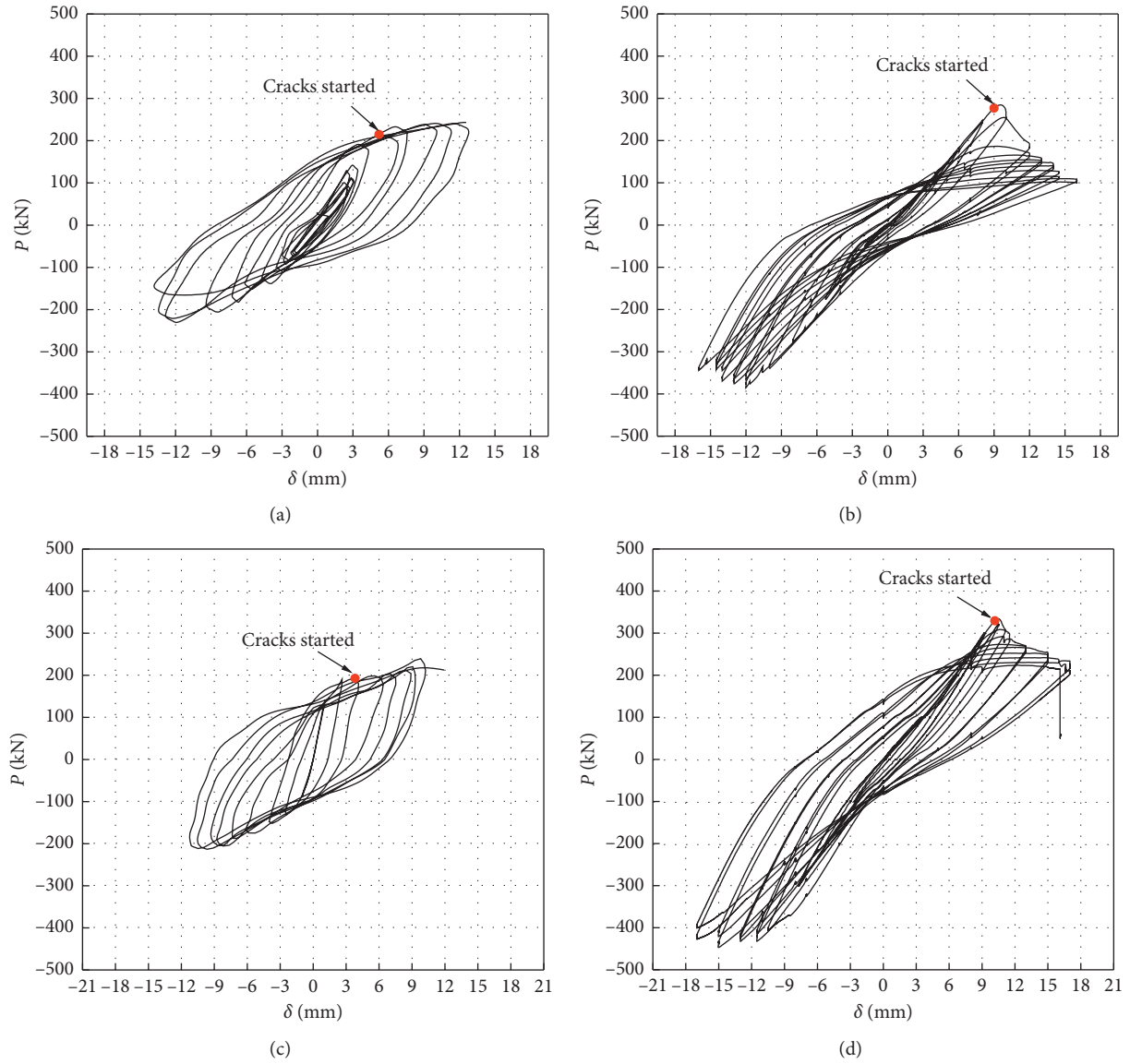

Figure 6: The hysteretic curves of the joints. (a) K-RC, (b) K-RC1, (c) K-CC, and (d) K-CC1.

Table 3: The control load and displacement ductility coefficient of joints.

Specimen	Tension		Compression		r_t (%)	r_c (%)	δ_u (mm)	δ_y (mm)	μ
	P_u (kN)	P_y (kN)	P_u (kN)	P_y (kN)					
K-RC	245.1	198.2	−230.5	−190.8	—	—	13.5	6.1	2.21
K-RC1	286.2	260.5	−376.8	−328.7	16.8	63.5	16.4	9.7	1.69
K-CC	240.2	168.3	−221.9	−172.5	—	—	12.5	5.6	2.23
K-CC1	334.5	312.8	−432.7	−389.2	13.9	95.0	17.1	10.2	1.68

In equation (3), n is the number of times of cyclic loading, E_i^+ and E_i^- are the energy dissipations under tension and compression in the ith loading, respectively. E_y is the nominal elastic potential energy of overlapped K-joints [1], which can be calculated by the yield load P_y and yield displacement δ_y in Figure 7.

The results of the energy dissipation of the overlapped K-joints are shown in Table 4. η_a and h_e of reinforced K-joints are smaller than those of unreinforced K-joints. In addition, the h_e of the unreinforced K-joints under collaborative cyclic loading is close to 0.3, which indicates that the unreinforced K-joints have good energy dissipation capability. The cumulative energy dissipation coefficients (E_T) of the reinforced K-joints are higher than those of the unreinforced joints. On the contrary, the accumulative energy dissipation ratio (η) of the unreinforced K-joints is

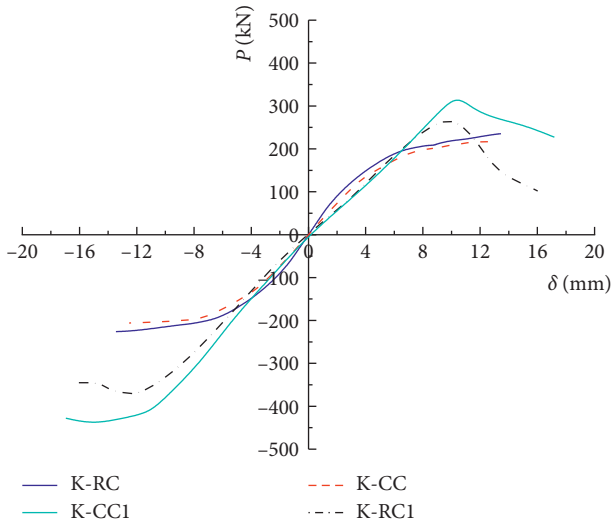

Figure 7: The skeleton curve.

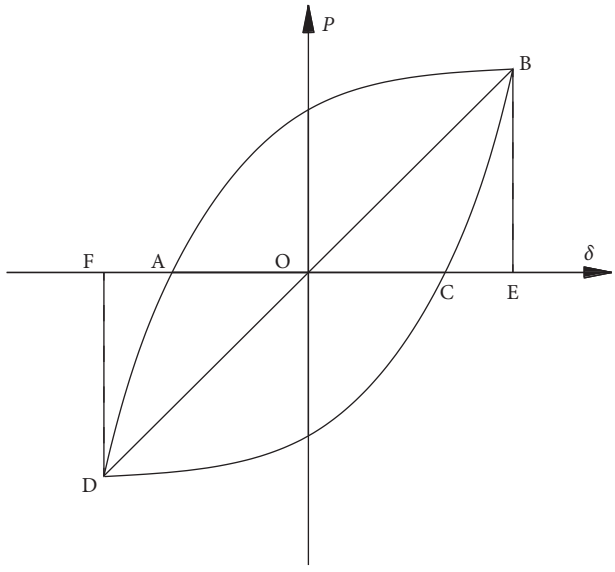

Figure 8: Typical hysteretic curve.

greater than that of the reinforced joints. For instance, the accumulative energy dissipation ratio of the K-RC is 92.2% higher than that of the joint K-RC1 and the K-CC is 100.5% higher than for the K-CC1. As far as the section form of the chord is concerned, the accumulative energy dissipation ratio (η) of K-RC is 6.5% smaller than that of K-CC, while the accumulative energy dissipation ratio (η) of K-RC1 is 8.5% higher than that of K-CC1, even if the strengthening measures of adding double plate effectively has improved the ultimate bearing capacity of overlapped K-joints. However, the effect of this strengthening method on the seismic performance of overlapped K-joints is different. The energy dissipation capacity of reinforced joints is smaller than the unreinforced joints.

Based on the cumulative energy dissipating coefficient E_T in Table 4, the relationship curve between the cumulative energy dissipating coefficient and displacement is obtained, as shown in Figure 9. The longitudinal axis is the cumulative energy dissipating coefficient E_T, which corresponds to the cumulative energy consumption under this displacement and the transverse axis is the average of the absolute values of compression and tension displacement. Figure 9 shows that the energy dissipating coefficient E_T of the joints is small before yielding and increases as the displacement increases, which indicates that the energy dissipating capacity of the joint is poor. After the yielding occurred, the energy dissipating coefficient of the joint became bigger gradually with the increase of control displacement, which indicates that the joint has excellent plastic energy dissipating capacity.

3.5. Load Transfer and Failure Mechanism. As stated above, failure modes, hysteretic performance, bearing capacity, and ductility of joints vary with the presence of double plates. To clarify the influence of double plates on the mechanical properties of K-joints in detail, K-RC and K-RC1 are selected to analyze and compare their load transfer schematics in Figure 10. Because all the failures of specimens were caused by cracking under tension, the load transfer path of the through brace under tension load is discussed. The force transfer schematics of the joints with circular chord are similar to that of the joints with the square chord. As shown in Figure 10, only the transfer schematics of K-joints with square chord were given.

In terms of the unreinforced K-joint, the tensile load on the through brace is decomposed into horizontal and vertical directions, both of which are $0.707P$ in magnitude. Then, the vertical force acts directly on the upper surface of the chord. Meanwhile, the overlap brace is in state of compression. Ultimately, because the radial stiffness of the chord is weak, concave, and convex deformations occur on the surface of a square steel tube. At this time, the damage of the weld between the through and the overlap brace is not obvious, only small cracks appear. For the reinforced joint K-RC1, it is different from the load transfer mechanism of K-RC. Because there is the double plate between the chord and the brace of K-RC1, so the load is transferred by the double plate. Since the plate is connected to the chord by the surrounding weld, the load is transmitted to the chord through the weld. When the through brace is subjected to an upward load, the weld is subjected to an eccentric load in the vertical direction, which is also the cause of the additional bending moment. Therefore, hysteretic performance and failure modes of joints are inevitably affected by the double plate. On the one hand, because of the presence of the double plate, the additional bending moments M are generated at the connection between the through brace and the double plate when the through brace is stretched, as shown in Figure 10(b). On the other hand, compressed overlapped brace and tensioned through brace are subjected to a force of $0.707P$ equal in size and opposite in direction, which means that the weld between the through and the overlap braces is subjected to vertical upward and downward forces with $0.354P$ in size, respectively. In summary, the two factors stated above both contribute to the cracking and expansion of weld between the through and the overlapped brace,

Table 4: Energy dissipation details of the joints.

Specimen	$S_{(ABC+CDA)}$ (kN·mm)	$S_{\Delta(OBE+ODF)}$ (kN·mm)	η_a	h_e	E_T (kN·mm)	E_y (kN·mm)	η
K-RC	4862.8	2796.5	1.74	0.278	22369.7	605.6	36.9
K-RC1	3720.6	5168.6	0.72	0.115	27319.5	1428.9	19.2
K-CC	4510.4	2684.7	1.68	0.268	19176.5	486.8	39.34
K-CC1	5848.7	6410.8	0.91	0.145	31554.6	1787.8	17.7

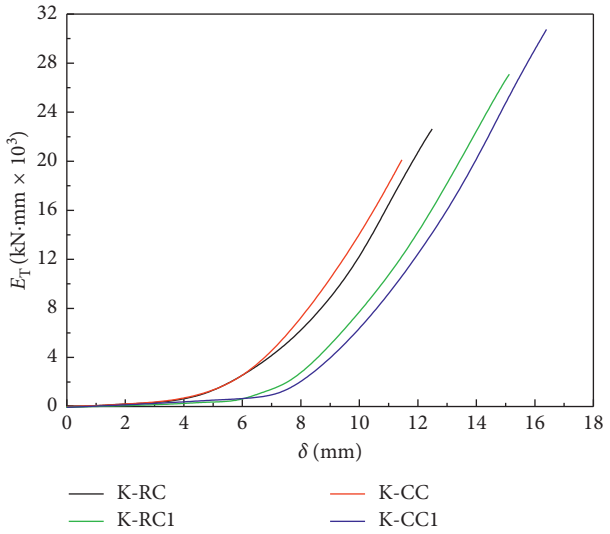

Figure 9: The relationship curve of E and displacement.

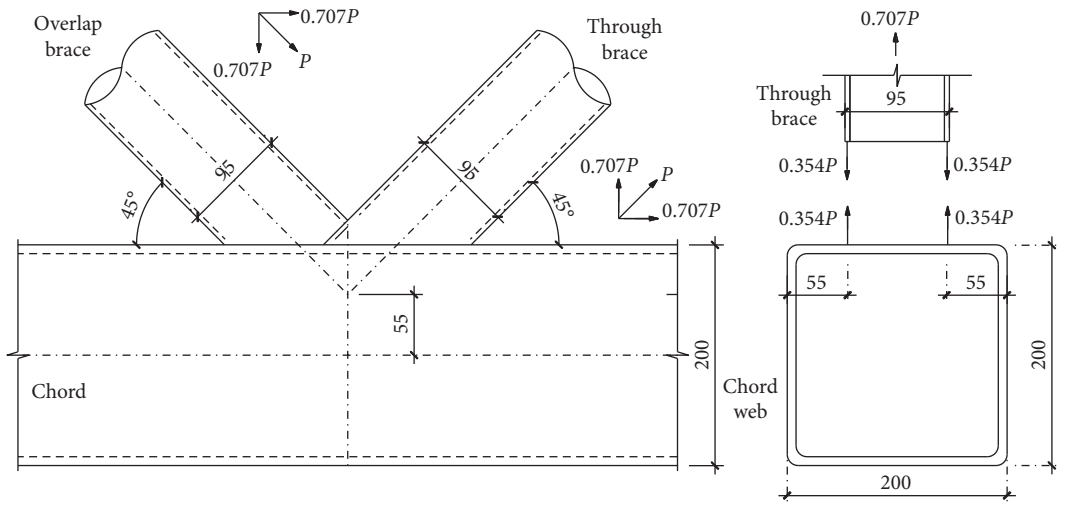

(a)

Figure 10: Continued.

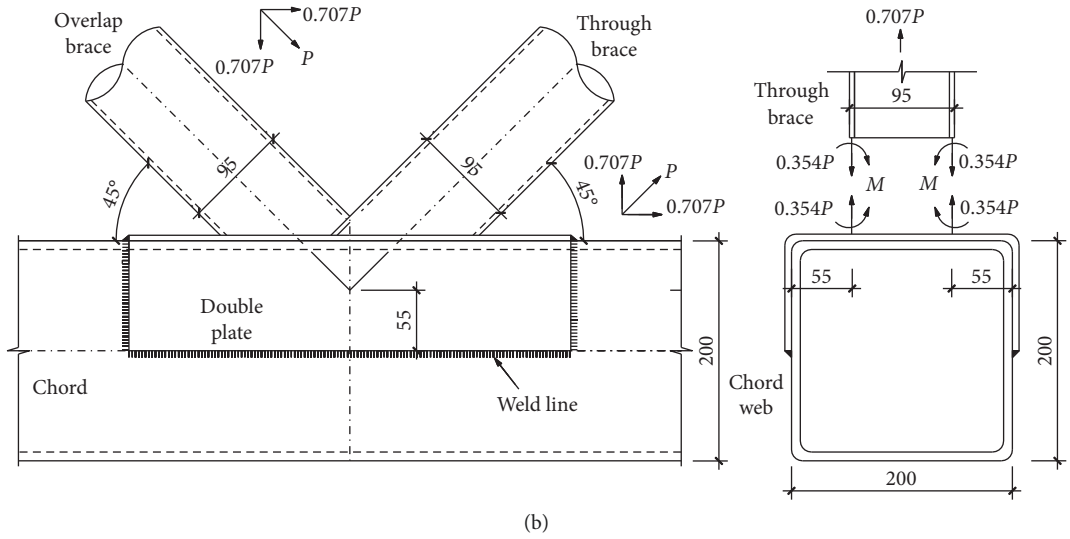

Figure 10: The load transfer mechanism of the through brace under tension. (a) K-RC and (b) K-RC1.

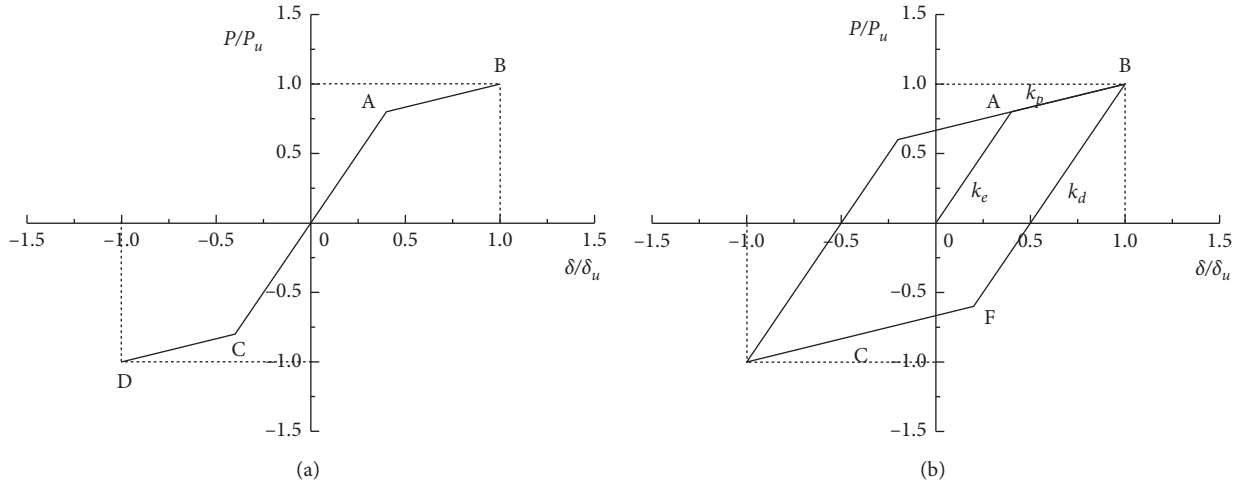

Figure 11: Loading and unloading stiffness of the joints.

which is in good agreement with the failure mode of the strengthened joints shown in Figure 5.

4. Restoring Force Model of K-Joints

The Clough [47] model and the Takeda [48] model are the classical restoring force models in the field of seismic engineering. Based on the existing restoring force model, the hysteretic curve of the joint is fitted by an envelope curve. Firstly, the fitted skeleton curves are shown in Figure 11. The dimensionless parameter δ/δ_u is defined as the transverse axis and P/P_u is defined as the longitudinal axis. P_u represents the ultimate bearing capacity of joints and δ_u is the ultimate displacement of joints under the cyclic loading. As shown in Figure 11, the skeleton curve of the joints is a double-folding line model and the joints undergo elastic and strengthening stages under the cyclic loading. The restoring force model of joints is shown in Figure 12 and the polyline function expression of the restoring force model is as follows:

$$\text{Line segment 0A: } \frac{P}{P_u} = k_e \frac{\delta}{\delta_u}, \quad |P| \le P_y, \tag{6}$$

$$\text{Line segment AB: } \frac{P}{P_u} = k_p \frac{\delta}{\delta_u} + \alpha, \quad P_u \ge |P| \ge P_y, \tag{7}$$

$$\text{Line segment BF: } \frac{P}{P_u} = k_d \frac{\delta}{\delta_u} + \beta, \quad P_u \ge |P| \ge P_y, \tag{8}$$

where k_e denotes the elastic stiffness of joints; k_p denotes the elastoplasticity stiffness of joints; and k_d denotes the residual stiffness of joints after degenerating and is equal to the elastic stiffness k_e. According to the double-folding line model, the loading and unloading stiffness of the joints can be

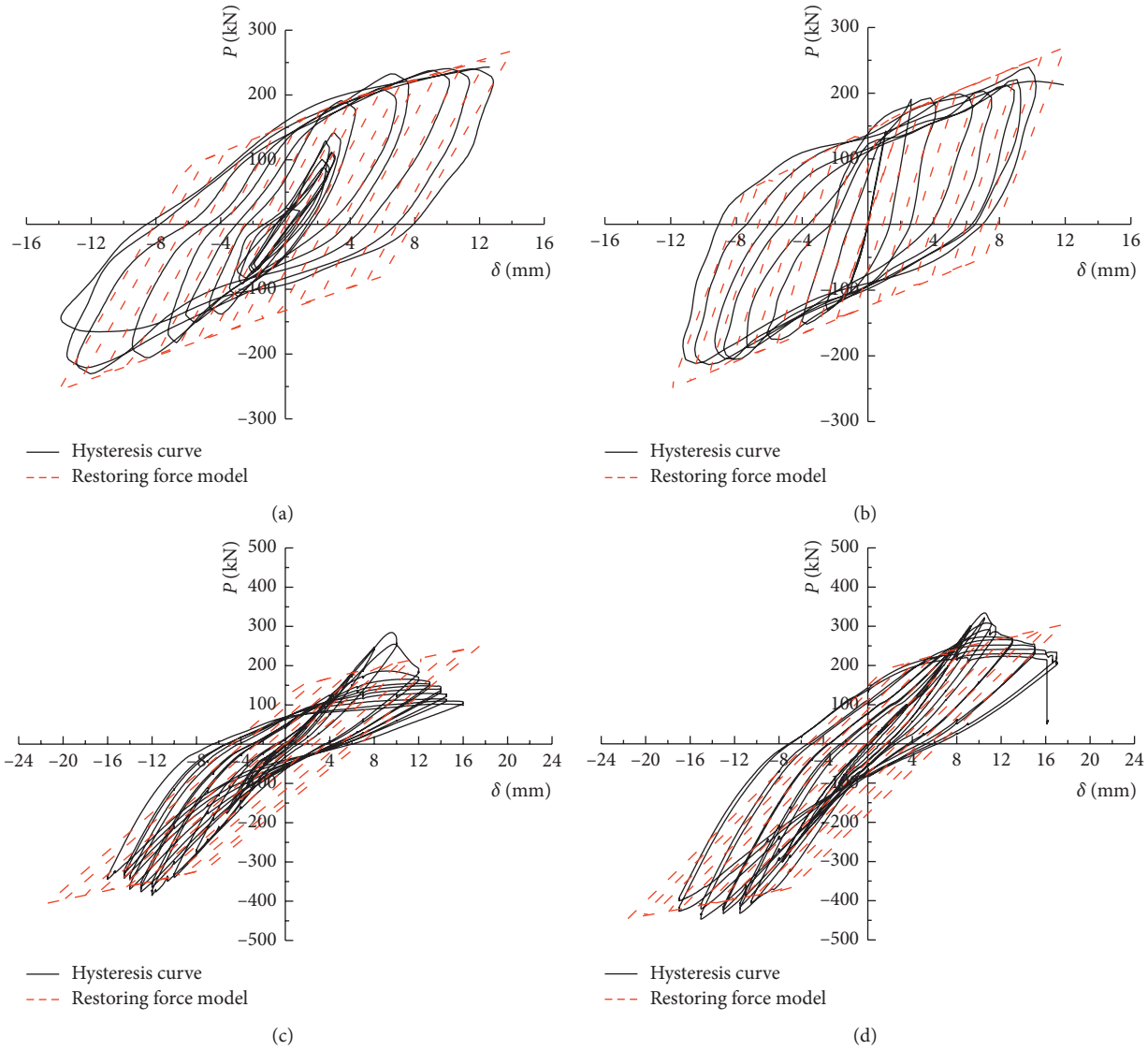

Figure 12: Restoring force model of the joints. (a) K-RC, (b) K-CC, (c) K-RC1, and (d) K-CC1.

calculated by fitting the hysteretic curve obtained from the test. Finally, the restoring force model of joints is proposed, which can be seen in Figure 12.

As shown in Figure 12, the coincidence degree between the restoring force models of unreinforced joints and the hysteretic curves obtained from tests is higher than that of reinforced joints. In terms of the double-plate reinforced K-joints, although the bearing capacity of joints has been improved obviously due to the existence of the double plate, the opening of welds is not conducive to the improvement of tensile strength. Based on this situation, the restoring force models of the reinforced joints is modified and the ultimate tensile strength of reinforced joints is reduced by 30%, which caused that the compressed capacity of reinforced joints is higher than the tensile capacity of reinforced joints. Therefore, the restoring force models of reinforced joints will not assume a symmetrical shape; as a whole, which is consistent with the results of the test above. As shown in Table 5, the average values of the absolute values of the tension and compression bearing capacity are taken as the bearing capacity of the joints. The difference between the model results and the test results is not more than 13.0%. Compared to the unreinforced joints, the bearing capacity of the reinforced joints in test is smaller than that of the restoring force models. But the error between them is less than 2%. It shows that the restoring force model is reliable for the double-plate reinforced overlapped K-joints.

5. Conclusions

The quasistatic loading scheme was adopted to carry out the reciprocating loading tests for the four overlapped K-joints along the axis of the brace. The experimental results and the restoring force model are compared and analyzed. Influence of the double-plate reinforced stress on the failure mode and

Table 5: Comparison between test results and model results.

Specimen	Test results (kN)			Model results (kN)			Error (%)
	Tension	Compression	Average	Tension	Compression	Average	
K-RC	245.1	−230.5	237.8	270.2	−254.7	262.5	10.3
K-RC1	286.2	−376.8	331.5	251.6	−404.2	327.9	1.1
K-CC	240.2	−221.9	231.1	268.1	−252.1	260.1	12.5
K-CC1	334.5	−432.7	383.6	313.6	−443.8	378.7	1.3

hysteretic behavior of the joints was explored. The conclusions are as follows:

(1) Failure of unreinforced joints occurs at the weld position on the chord surface and the tiny cracks appeared along the weld. For the K-RC1 joint, cracks appeared at the junction weld between the through brace and the overlap brace. However, cracks extended along with the weld at the intersection of the chord and the through brace for K-CC1. There is no obvious deformation on the chord surface of reinforced joints.

(2) The double-plate reinforced measures effectively restrain the plastic deformation of the chord and avoid the large stress concentration of the chord in the intersecting area of the brace and chord. The ultimate capacity (P_u) in tension of K-RC1 and K-CC1 are, respectively, 16.8% and 13.9% higher than the corresponding unreinforced joints. The ultimate capacity (P_u) in compression of K-RC1 and K-CC1 are 63.5% and 95.0% higher than the corresponding unreinforced joints. But the double-plate reinforced measures reduce the ductility of the joint by 30%. In addition, compared to the unreinforced joints, energy dissipation capacity of reinforced joints is smaller.

(3) According to the double-folding line model, the loading and unloading stiffness of the joints can be calculated by fitting the hysteretic curve obtained from the test. And, based on the test results, the restoring force model of joints is proposed. The error between the bearing capacity of the reinforced joints in the test and the restoring force model is less than 2%. It shows that the restoring force model is reliable for the double-plate reinforced overlapped K-joints

Data Availability

The data used to support the findings of this study are available from the corresponding author upon request.

Conflicts of Interest

The authors declare no conflicts of interest.

Authors' Contributions

Wenwei Yang and Shuntao Li are co-first authors. W.Y. incepted the original idea and designed the experiment. S.L. and R.Y. analyzed the data and wrote the paper. W.Y. and Y.S. revised the paper.

Acknowledgments

This research was supported in part by the Natural Science Foundation Project of Ningxia Province (no. 2019AAC03004) and in part by the Funding Project of First-Class Discipline Construction of Universities in Ningxia (Domestic First-Class Discipline Construction) under Grant NXYLXK2017A03.

References

[1] W. Yang, R. Yan, Y. Suo, G. Zhang, and B. Huang, "Experimental study on hysteretic behavior of the overlapped k-joints with concrete filled in chord," *Applied Sciences*, vol. 9, no. 7, p. 1456, 2019.

[2] A. Gillman, K. Fuchi, and P. Buskohl, "Truss-based nonlinear mechanical analysis for origami structures exhibiting bifurcation and limit point instabilities," *International Journal of Solids and Structures*, vol. 147, pp. 80–93, 2018.

[3] F. Gao, Z. Xiao, X. Guan, H. Zhu, and G. Du, "Dynamic behavior of CHS-SHS tubular T-joints subjected to low-velocity impact loading," *Engineering Structures*, vol. 183, pp. 720–740, 2019.

[4] W. Li, T. Liu, J. Wang, D. Zou, and S. Gao, "Finite-element analysis of an electromechanical impedance–based corrosion sensor with experimental verification," *Journal of Aerospace Engineering*, vol. 32, no. 3, Article ID 04019012, 2019.

[5] L. Huo, C. Li, T. Jiang, and H.-N. Li, "Feasibility study of steel bar corrosion monitoring using a piezoceramic transducer enabled time reversal method," *Applied Sciences*, vol. 8, no. 11, p. 2304, 2018.

[6] S. Arabi, B. Shafei, and B. M. Phares, "Investigation of fatigue in steel sign-support structures under diurnal temperature changes," *Journal of Constructional Steel Research*, vol. 153, pp. 286–297, 2019.

[7] S.-Z. Qu, X.-H. Wu, and Q. Sun, "Experimental and numerical study on ultimate behaviour of high-strength steel tubular K-joints with external annular steel plates on chord circumference," *Engineering Structures*, vol. 165, pp. 457–470, 2018.

[8] Eurocode 3 (EC3), *Design of Steel Structures—Part 1–8: Design of Joints (EN 1993-1-8)*, European Committee for Standardization, Brussels, Belgium, 2005.

[9] J. A. Packer, J. Wardenier, Y. Kurobane et al., *Design Guide for Rectangular Hollow Section (RHS) Joints under Predominantly Static Loading*, Comité International pour le Développement et l'Étude de la Construction Tubulaire (CIDECT), Cologne, Germany, 1992.

[10] W. Huang, L. Fenu, B. Chen, and B. Briseghella, "Experimental study on K-joints of concrete-filled steel tubular truss

structures," *Journal of Constructional Steel Research*, vol. 107, pp. 182–193, 2015.

[11] X. Zhao, J. Liu, X. Xu, K. S. Sivakumaran, and Y. Chen, "Hysteretic behaviour of overlapped tubular k-joints under cyclic loading," *Journal of Constructional Steel Research*, vol. 145, pp. 397–413, 2018.

[12] X. L. Wang, W. W. Yang, and L. Zou, "Finite element analysis for unstiffened overlapped CHS K-joints welded in different ways," *Advanced Materials Research*, vol. 163–167, pp. 299–306, 2010.

[13] Chinese Code (GB/50017-2017), *Standard for Design of Steel Structures*, Standards Press of China, Beijing, China, 2017.

[14] G. Du, A. Andjelic, Z. Li, Z. Lei, and X. Bie, "Residual axial bearing capacity of concrete-filled circular steel tubular columns (CFCSTCs) after transverse impact," *Applied Sciences*, vol. 8, no. 5, p. 793, 2018.

[15] B. Zhao, H. Zhu, Y. Yin, Z. Liu, and Q. Han, "Structural behaviour of an assembled steel joint composed of CHS KK-joint and doubler plate for connection with steel tensile rods," *International Journal of Steel Structures*, vol. 18, no. 2, pp. 674–684, 2018.

[16] Ö. Zeybek, C. Topkaya, and J. M. Rotter, "Strength and stiffness requirements for intermediate ring stiffeners on discretely supported cylindrical shells," *Thin-Walled Structures*, vol. 96, pp. 64–74, 2015.

[17] L. H. Han, L. Q. Zheng, S. H. He, and Z. Tao, "Tests on curved concrete filled steel tubular members subjected to axial compression," *Journal of Constructional Steel Research*, vol. 67, no. 6, pp. 965–976, 2011.

[18] F.-X. Ding, L. Luo, L. Wang, S. Cheng, and Z.-W. Yu, "Pseudo-static tests of terminal stirrup-confined concrete-filled rectangular steel tubular columns," *Journal of Constructional Steel Research*, vol. 144, pp. 135–152, 2018.

[19] G. Du, Z. Li, and G. Song, "A PVDF-based sensor for internal stress monitoring of a concrete-filled steel tubular (CFST) column subject to impact loads," *Sensors*, vol. 18, no. 6, p. 1682, 2018.

[20] Y. Shi, M. Luo, W. Li, and G. Song, "Grout compactness monitoring of concrete-filled fiber-reinforced polymer tube using electromechanical impedance," *Smart Materials and Structures*, vol. 27, no. 5, Article ID 055008, 2018.

[21] P. Gandhi, G. Raghava, and D. R. Murthy, "Fatigue behavior of internally ring-stiffened welded steel tubular joints," *Journal of Structural Engineering*, vol. 126, no. 7, pp. 809–815, 2000.

[22] M. Lee and A. Llewelyn-Parry, "Offshore tubular T-joints reinforced with internal plain annular ring stiffeners," *Journal of Structural Engineering*, vol. 130, no. 6, pp. 942–951, 2004.

[23] M. M. Lee and A. Llewelyn-Parry, "Strength prediction for ring-stiffened DT-joints in offshore jacket structures," *Engineering Structures*, vol. 27, no. 3, pp. 421–430, 2005.

[24] Y. Yin, Q. Han, L. Bai, H. Yang, and S. Wang, "Experimental study on hysteretic behaviour of tubular N-joints," *Journal of Constructional Steel Research*, vol. 65, no. 2, pp. 326–334, 2009.

[25] N. V. Gomes, L. R. O. de Lima, P. C. G. S. Vellasco et al., "Experimental and numerical investigation of SHS truss T-joints reinforced with sidewall plates," *Thin-Walled Structures*, vol. 145, Article ID 106404, 2019.

[26] L. R. O. de Lima, L. C. B. Guerrieiro, P. C. G. S. Vellasco et al., "Experimental and numerical assessment of flange plate reinforcements on square hollow section T joints," *Thin-Walled Structures*, vol. 131, pp. 595–605, 2018.

[27] Y. Kurobane, Y. Makino, and K. Ochi, "Ultimate resistance of unstiffened tubular joints," *Journal of Structural Engineering*, vol. 110, no. 2, pp. 385–400, 1984.

[28] X. Zhao, Y. Chen, Y. Chen, G. Wang, L. Xu, and R. Zhang, "Experimental study on static behavior of unstiffened, overlapped CHS K-joints," *Jianzhu Jiegou Xuebao/Journal of Building Structures*, vol. 27, pp. 23–29, 2006.

[29] W.-B. Kim, "Ultimate strength of tube–gusset plate connections considering eccentricity," *Engineering Structures*, vol. 23, no. 11, pp. 1418–1426, 2001.

[30] J. A. Packer and J. Henderson, *Design Guide for Hollow Structural Section Connections*, Canadian Institute of Steel Construction, Willowdale, Ontario, Canada, 1992.

[31] M. Lesani, M. R. Bahaari, and M. M. Shokrieh, "Detail investigation on un-stiffened T/Y tubular joints behavior under axial compressive loads," *Journal of Constructional Steel Research*, vol. 80, pp. 91–99, 2013.

[32] Y. Ju and D. Wang, "Nonlinear finite element analysis of the ultimate strength of tubeangle combo tower K-joints," *Strength of Materials*, vol. 47, pp. 355–361, 2015.

[33] B. H. Lv, Z. Q. Chen, H. Li, S. Q. Guan, X. L. Li, and L. Zhang, "Research on the ultimate bearing capacity for steel tubular transmission tower's joints with annular plate," *Applied Mechanics and Materials*, vol. 166–169, pp. 379–384, 2012.

[34] Z. J. Rong, X. M. Wang, B. H. Lv, X. Y. Zhang, and L. Zhang, "Theoretical analysis on the ultimate bearing capacity for steel tubular transmission tower's joints with annular Plate," *Applied Mechanics and Materials*, vol. 664, pp. 175–181, 2014.

[35] X. Qian, Y. Zhang, and Y. S. Choo, "A load–deformation formulation for CHS X-and K-joints in push-over analyses," *Journal of Constructional Steel Research*, vol. 90, pp. 108–119, 2013.

[36] W. Gho and Y. Yang, "Parametric equation for static strength of tubular circular hollow section joints with complete overlap of braces," *Journal of Structural Engineering*, vol. 134, no. 3, pp. 393–401, 2008.

[37] M. M. Lee and F. Gazzola, "Design equation for offshore overlap tubular K-joints under in-plane bending," *Journal of Structural Engineering*, vol. 132, no. 7, pp. 1087–1095, 2006.

[38] B. Wang, G. Huo, Y. Sun, and S. Zheng, "Hysteretic behavior of steel reinforced concrete columns based on damage analysis," *Applied Sciences*, vol. 9, no. 4, p. 687, 2019.

[39] S. Shon, M. Yoo, and S. Lee, "An experimental study on the shear hysteresis and energy dissipation of the steel frame with a trapezoidal-corrugated steel plate," *Materials*, vol. 10, no. 3, p. 261, 2017.

[40] J. Zhang, Y. Li, Y. Zheng, and Z. Wang, "Seismic damage investigation of spatial frames with steel beams connected to L-shaped concrete-filled steel tubular (CFST) columns," *Applied Sciences*, vol. 8, no. 10, p. 1713, 2018.

[41] B. Wang, H. Dai, T. Wu, G. Bai, and Y. Bai, "Experimental investigation on seismic behavior of steel truss-RC column hybrid structure with steel diagonal braces," *Applied Sciences*, vol. 8, no. 1, p. 131, 2018.

[42] F. Qin, T. Fung, and C. Soh, "Hysteretic behavior of completely overlap tubular joints," *Journal of Constructional Steel Research*, vol. 57, no. 7, pp. 811–829, 2001.

[43] C. Soh, T. Fung, F. Qin, and W. Gho, "Behavior of completely overlapped tubular joints under cyclic loading," *Journal of Structural Engineering*, vol. 127, no. 2, pp. 122–128, 2001.

[44] W. Wang and Y.-Y. Chen, "Hysteretic behaviour of tubular joints under cyclic loading," *Journal of Constructional Steel Research*, vol. 63, no. 10, pp. 1384–1395, 2007.

[45] Chinese Code (JGJ81-2002), *Technical Specification for Welding of Steel Structure of Building*, Standards Press of China, Beijing, China, 2003.
[46] Chinese Code (GB/T 228-2002), *Metallic Materials-Tensile Testing at Ambient Temperature*, Standards Press of China, Beijing, China, 2002.
[47] R. W. Clough, "Effect of stiffness degradation on earthquake ductility requirements," in *Proceedings of the Japan Earthquake Engineering Symposium*, Tokyo, Japan, 1966.
[48] T. Takeda, M. A. Sozen, and N. N. Nielsen, "Reinforced concrete response to simulated earthquakes," *Journal of the Structural Division*, vol. 96, pp. 2557–2573, 1970.